Journal of the American College of Cardiology Vol. 45, No. 3, 2005

Published by Elsevier Inc.
ISSN 0735-1097/05/$30.00
doi:10.1016/j.jacc.2004.10.040

Multislice Computed Tomography Versus Intracardiac Echocardiography to Evaluate the Pulmonary Veins Before Radiofrequency Catheter Ablation of Atrial Fibrillation

A Head-to-Head Comparison

Monique R. M. Jongbloed, MD,* Jeroen J. Bax, MD, PHD,* Hildo J. Lamb, MD, PHD,† Martijn S. Dirksen, MD, PHD,† K. Zeppenfeld, MD, PHD,* Ernst E. van der Wall, MD, PHD,* Albert de Roos, MD, PHD,† Martin J. Schalij, MD, PHD*

Leiden, the Netherlands

OBJECTIVES The purpose of this study was to perform a head-to-head comparison between multislice computed tomography (MSCT) and intracardiac echocardiography (ICE).

BACKGROUND Different imaging techniques have been used to visualize the pulmonary veins (PV) before radiofrequency ablation of atrial fibrillation.

METHODS The PV and their atrial insertion were evaluated in 42 patients (35 men, 49 ± 9 years) admitted for ablation of PV ostia. Ostia were measured in two directions (anterior-posterior and superior-inferior) with MSCT. Two-dimensional (2-D) measurements of PV ostia were performed with ICE. Results were compared, considering MSCT as the gold standard. Venous ostium indexes were calculated by dividing MSCT measurements in the anterior-posterior direction and the superior-inferior direction.

RESULTS Common ostia of left PV were observed in 33 (79%) patients with MSCT and 31 (74%) patients with ICE. Common ostia of right PV were observed in 13 (31%) and 16 (38%) patients, respectively. Additional PV were observed in 13 (31%) patients with MSCT and in 7 (17%) patients with ICE. Ostial diameters by MSCT in the anterior-posterior direction were similar to 2-D measurements by ICE. By contrast, diameters by MSCT in the superior-inferior direction were significantly larger than 2-D diameters measured with ICE. Venous ostium indexes were 0.77 ± 0.18 and 0.90 ± 0.15 ($p < 0.01$) for left and right PV respectively, indicating an oval shape of particularly left PV ostia.

CONCLUSIONS Variation in PV anatomy is frequently observed with both techniques. The sensitivity for detection of additional branches is higher for MSCT. Results of measurements of PV ostia suggest an underestimation of ostial size by ICE. Three-dimensional imaging techniques, such as MSCT, are required to demonstrate an oval shape of PV ostia. (J Am Coll Cardiol 2005;45:343–50) © 2005 by the American College of Cardiology Foundation

Radiofrequency catheter ablation (RFCA) is a potentially curative treatment modality for atrial fibrillation originating in the pulmonary veins (PV) (1). The RFCA for atrial fibrillation can be aimed at either eliminating ectopic pulmonary venous foci (2,3) or at electrical isolation of PV (4). For proper targeting of radiofrequency lesions, accurate visualization and knowledge about PV anatomy is necessary. Fluoroscopy alone cannot provide sufficient information on intracardiac anatomic structures such as the pulmonary venous ostia.

In recent years, the value of different imaging techniques to guide RFCA procedures has been recognized. For the acquisition of anatomic information of PV anatomy before RFCA, three-dimensional (3-D) imaging techniques, such as multislice computed tomography (MSCT), have been applied (5). Multislice computed tomography has proved to be able to provide accurate and detailed information of PV anatomy (6).

On-line acquisition of anatomic information regarding left atrial and PV anatomy can also be obtained by intracardiac echocardiography (ICE) (7,8). Advantages of this imaging technique include the possibility to obtain on-line information of left atrial anatomy and PV in relation to ablation catheters, potential to assess hemodynamic function and the monitoring of acute complications, such as pericardial effusion and acute PV stenosis.

Thus, both MSCT and ICE can be used for imaging of the PV and their ostia before RFCA, and to obtain quantitative information. To date, there is limited information on the comparison between MSCT and ICE. In the current study, considering MSCT as the gold standard, we have compared the ability of both techniques to: 1) provide anatomic information regarding PV anatomy in patients admitted for PV isolation for atrial fibrillation, and 2) compare measurements of the ostia of the PV in two directions obtained with MSCT with two-dimensional (2-D) measurements obtained with ICE.

From the Departments of *Cardiology and †Radiology, Leiden University Medical Center, Leiden, the Netherlands.

Manuscript received June 18, 2004; revised manuscript received September 20, 2004, accepted October 4, 2004.

JACC Vol. 45, No. 3, 2005
February 1, 2005:343–50

Abbreviations and Acronyms

ICE = intracardiac echocardiography
MSCT = multislice computed tomography
PV = pulmonary veins
RFCA = radiofrequency catheter ablation
2-D = two-dimensional
3-D = three-dimensional

PATIENTS AND METHODS

Study population. The study population consisted of 42 consecutive patients (35 men, age 49 ± 9 years, range 24 to 68 years) with symptomatic drug-refractory atrial fibrillation, admitted for RFCA aimed at electrical isolation of the PV by the application of radiofrequency current at the pulmonary venous ostia. Mean duration of atrial fibrillation was 5 ± 4 years (range 1 to 25 years). Atrial fibrillation was paroxysmal in 28 patients, persistent in 10, and permanent in 4 patients. Mean left atrial size was 4.4 ± 0.8 cm. Mean number of anti-arrhythmic drugs used was 3.8 ± 1.6 per patient. Mean left ventricular ejection fraction was 62.8 ± 9.6%. Thirteen patients had a history of heart failure (New York Heart Association functional class 1 to 2); heart failure was due to tachycardia-induced cardiomyopathy in 5 of these patients. One patients had a history of coronary artery disease; in 14 patients mild valvular disease was present (mitral regurgitation grade 1 to 2). Four patients had a pacemaker.

MSCT. The MSCT was performed using a Toshiba Multi-slice Aquilion system (Toshiba Medical Systems, Otawara, Japan), with either a 4-slice (16 patients) or a 16-slice (26 patients) system two days before RFCA. Non-ionic contrast material (Xenetix 300, Guerbet, Aulnay S. Bois, France) was injected in the antebrachial vein (160 ml, flow rate 4.0 ml/s). Craniocaudal scanning (coverage length 80 to 120 mm) was performed at the level of the atria using simultaneous acquisition of 4 sections with a collimated slice thickness of 2 mm or 16 sections with a collimated slice thickness of 0.5 mm, respectively. Helical pitch was 1 mm/0.5 s for the 4-slice scanner and 4 mm/0.5 s for the 16-slice scanner. For the 16-slice scanner, rotation time was 400 to 600 ms (dependent on the patient's heart rate) and tube voltage was 120 kV at 250 mA. Scanning was performed during breath-holding. A segmental reconstruction algorithm was used to allow for the inclusion of patients with a range of heart rates. Retrospective electrocardiographic gating was performed to eliminate cardiac motion artefacts. Data acquisition was completed in 20 s. Data reconstruction was performed on a Vitrea post-processing workstation (Vital Images, Plymouth, Minnesota) with use of 2-D viewing modes and 3-D reconstructions.

Reconstructions were evaluated in three different orthogonal planes (transversal, sagittal, and coronal) or with angulated multiplanar reformat. In addition, PV anatomy was evaluated using 3-D reconstructions.

ICE. Intracardiac echocardiography was performed with an Acunav Diagnostic Ultrasound Catheter, connected to a Sequoia ultrasound system (Acuson Corporation, Mountain View, California). The ultrasound catheter consists of a miniaturized 64-element, monoplane phased-array transducer, which is incorporated in a 10-F single use catheter. This catheter was positioned in the right atrium through the left femoral vein. On initiation of each RFCA procedure, PV anatomy was explored with ICE and measurements of PV ostia were performed.

Definitions. For the evaluation of the pulmonary venous ostia, the following definitions were used:

MSCT. A line following the outer contour of the left atrium was drawn in different orthogonal planes to determine whether there was a separate or common insertion of the PV in the left atrium. If the pulmonary venous ostia entered the left atrium separately outside this line, the ostia were defined as being "separate ostia" (Fig. 1). When the PV united before entering the drawn outer left atrial contour in the transversal, coronal, and sagittal orthogonal plane, the ostium was defined as a "common ostium" (Fig. 2). "Additional PV" were defined as entering the left atrium in separate ostia. "Early branching" was defined as branching of the PV within 1 cm of the bifurcation of the PV.

ICE. Similar to MSCT, the site of the atriovenous border was determined by extrapolation of the outer border of the left atrium, and a line was drawn at the junction of the PV with the left atrium. If atrial tissue could be distinguished between the ostia of both PV, the ostia were defined as "separate ostia." When a common truncal part was present before entering this line, the ostia were defined as "common ostia" (Fig. 3). For right PV, evaluation of ostia was not always possible in this way, as the right PV are situated in close proximity with the interatrial septum and often make a sharp angle with this structure. Therefore, it is not always possible to obtain longitudinal views, as is possible for the left PV. When the ICE transducer was positioned at the bifurcation of both right PV and a common trunk could be visualized, then the ostia of the right PV were defined as "common ostia." Similar to MSCT, "additional PV" enter the left atrium in separate ostia and "early branching" was defined as branching of the PV within 1 cm of the bifurcation of the PV.

Quantitative measurements. MSCT. For MSCT, measurements of the PV ostia in two directions were obtained, being: 1) the anterior-posterior direction, and 2) the superior-inferior direction. Multiplanar reformatting was used to obtain these measurements in two perpendicular directions (Fig. 4). Furthermore, the ratio between these measurements, the venous ostium index, was calculated to obtain information on the shape of the ostium. The more the venous ostium index deviates from the value 1, the more asymmetrical the shape of the ostium.

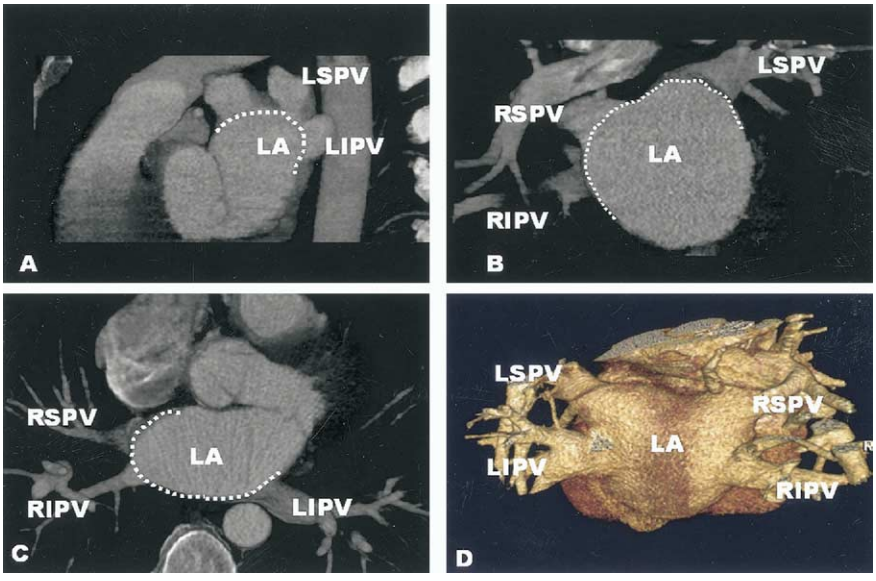

Figure 1. Evaluation of pulmonary venous ostial insertion in three different orthogonal planes in a patient with separate insertion of both left and right pulmonary veins in the left atrium. The **dotted line** depicts the extrapolated outer left atrial border. **(A)** Sagittal plane. Both left pulmonary veins enter the left atrium separately. **(B)** Coronal plane and **(C)** transversal plane. **(D)** Three-dimensional reconstruction. No common truncal part is observed in any plane before the veins enter the left atrium. Left atrial insertion of these veins was therefore designated as separate. LA = left atrium; LIPV = left inferior pulmonary vein; LSPV = left superior pulmonary vein; RIPV = right inferior pulmonary vein; RSPV = right superior pulmonary vein.

ICE. On the 2-D images obtained by ICE, the largest possible diameter of the PV ostium was measured (Figs. 3 and 4). Measurements of PV ostia by ICE were compared with both anterior-posterior diameters and superior-inferior diameters obtained with MSCT. All measurements were performed in consensus by two observers. The observers responsible for evaluation of the ICE data were blinded for the MSCT data and vice versa.

RFCA. The RFCA was aimed at electrical isolation of all PV from the left atrium by the circumferential application of ablation points aimed ±5 mm outside the ostium of the PV. Radiofrequency current was applied via a Stockert-Cordis (Freiburg, Germany) generator at each ablation point for 30 s, with maximum temperature setting at 60°C and maximum radiofrequency energy 50 W. Intracardiac echocardiography was used to exclude the presence of intracardiac thrombus, to guide transseptal puncture, and to evaluate the anatomy of the PV before RFCA. After the evaluation of the pulmonary venous anatomy and measurements of the ostia by ICE, the ablation strategy was planned using data obtained with both MSCT and ICE. If a separate pulmonary venous insertion was observed with

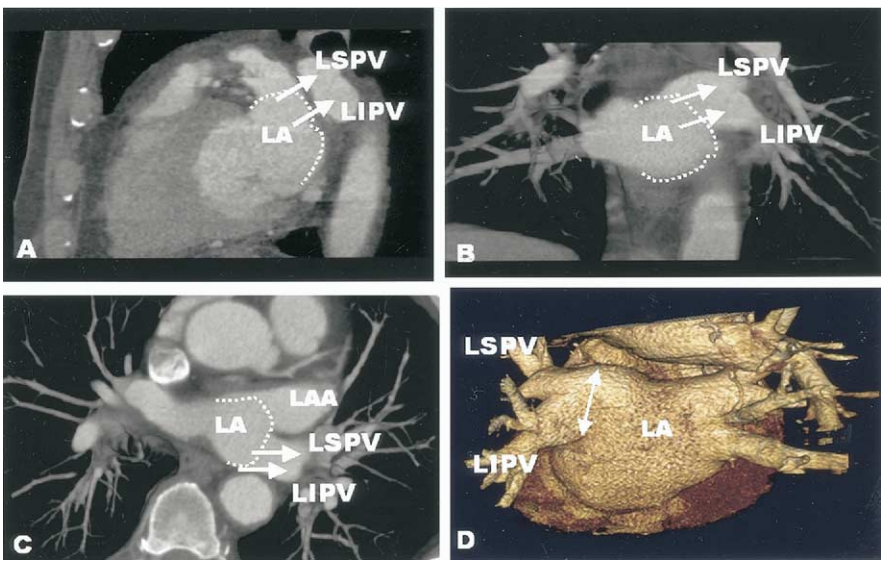

Figure 2. Common ostium of the left pulmonary veins, as evaluated in three different orthogonal planes and a three dimensional reconstruction using multislice computed tomography. **(A)** Sagittal plane. The superior and inferior pulmonary veins have united to form a common truncus before entering the left atrial body. **(B)** Coronal plane. **(C)** Transversal plane. **(D)** Three-dimensional reconstruction. A common truncus of the left pulmonary veins can be observed in all orthogonal planes and on the three-dimensional reconstruction. Abbreviations as in Figure 1.

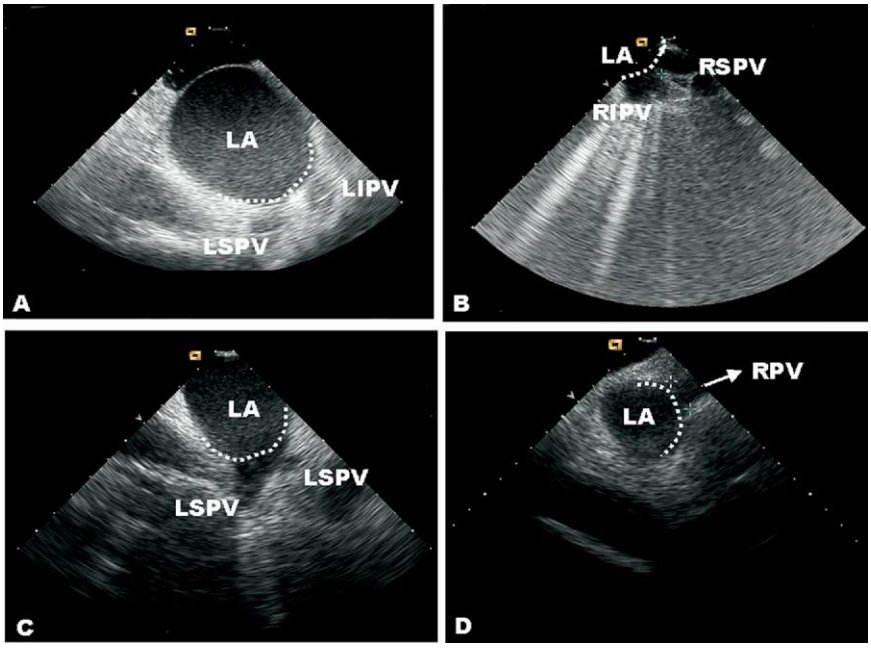

Figure 3. Method used to determine pulmonary vein ostial insertion in the left atrium using intracardiac echocardiography. The **dotted line** depicts the extrapolated outer left atrial border. **Panels A and B** represent separate insertion of left and right pulmonary veins, respectively, whereas **panels C and D** demonstrate a common ostium of the left and right pulmonary veins, respectively. Abbreviations as in Figure 1.

both techniques, radiofrequency current was targeted to form separate circles surrounding the pulmonary venous ostia. If a common ostium was observed with one or both techniques, ablation points were targeted in a large circle surrounding the common ostium. All additional PV observed were targeted as well. During the procedure, the MSCT scan was placed on a light panel opposite to the operator. On-line information obtained by ICE was used to monitor catheter navigation in the left atrium and to evaluate the position of the ablation catheter in relation to the ostia of the PV. When microbubbles were observed, the application of radiofrequency current was stopped and the catheter was repositioned in an attempt to provide better catheter-tip tissue contact. Furthermore, ICE was used to monitor the occurrence of acute complications during the procedure. A 3-D non-fluoroscopic mapping system

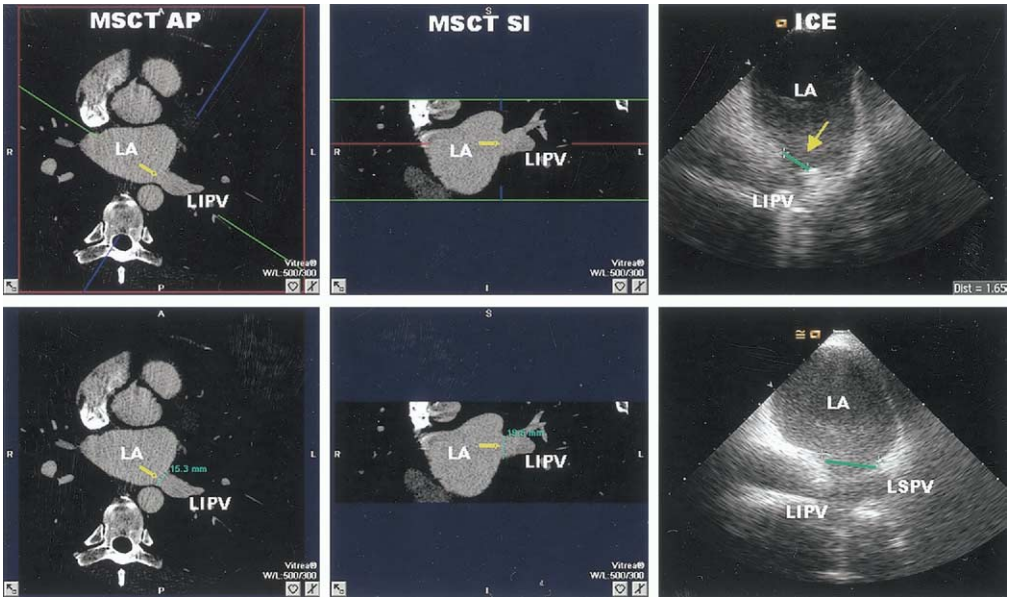

Figure 4. Measurements of the left inferior pulmonary vein (LIPV) with multislice computed tomography in two directions **(left and middle panels)** using multiplanar reformatting, and with intracardiac echocardiography **(right panel)**. **(Left panel)** Measurements in the anterior-posterior direction in the transversal orthogonal plane. The **green line** is placed parallel to the LIPV, and depicts the coronal plane, which is used to measure the ostium in the superior-inferior direction **(middle panel)**. **(Right panel)** Measurement of the LIPV **(upper panel)** and of a common ostium of the left pulmonary veins **(lower panel)** using intracardiac echocardiography. AP = anterior-posterior; SI = superior-inferior; other abbreviations as in Figure 1.

Table 1. Anatomic Results of MSCT Versus ICE

	MSCT	ICE
Total number of observed PV	181	175
Mean number of PV/pt	4.3 ± 0.6	4.2 ± 0.4
Pts with additional RPV	12 (29%)	7 (17%)
Pts with additional LPV	1 (3%)	0
Pts with early branching RPV	5 (12%)	5 (12%)
Pts with early branching LPV	35 (84%)	19 (45%)
Pts with common ostium RPV	13 (31%)	16 (38%)
Pts with common ostium LPV	33 (79%)	31 (74%)

ICE = intracardiac echocardiography; LPV = left pulmonary veins; MSCT = multislice computed tomography; Pts = patients; PV = pulmonary veins; RPV = right pulmonary veins.

(CARTO, Biosense Webster, Diamond Bar, California) was used to tag PV, to acquire electrophysiologic information, and to mark ablation points. Tagging of the PV was guided by the information of MSCT and ICE imaging, concerning number and insertion of PV. The procedure was designated successful when there was no capture in the PV and left atrium after pacing in the left atrium or PV, respectively and when the patient was in sinus rhythm after the procedure. All patients received heparin (activated clotting time 2 to 3 times baseline value, checked hourly).

Statistical analysis. Statistical analysis was performed using Microsoft Excel spreadsheets and SPSS 11.0 software for Windows. Data are expressed as mean ± SD. Diameters of PV ostia measured on-line with ICE before ablation were compared with measurements in the anterior-posterior direction performed with MSCT, and with measurements performed in the superior-inferior direction with MSCT, using the paired Student *t* test. This test was also used for comparisons between the measurements in two directions performed with MSCT. Bland Altman analysis was used to quantify the level of agreement between measurements with ICE and measurements with MSCT in both the anterior-posterior and superior-inferior directions. All tests were two-tailed, and a p value <0.05 was considered significant.

RESULTS

Pulmonary vein anatomy. In 42 patients, a total number of 181 PV was observed with MSCT and 175 PV with ICE. In all patients, at least four veins could be identified with both techniques (Table 1).

ADDITIONAL VEINS. Additional veins were observed more frequently on the right side with both ICE and MSCT. However, additional right veins were observed in 12 (29%) patients with MSCT as compared with 7 (17%) with ICE. Considering MSCT as the gold standard, the sensitivity of ICE to demonstrate additional right PV was 7 of 12 (58%). In one patient, an additional left PV was observed with MSCT, which was not recognized by ICE. Figure 5 (upper panel) demonstrates a MSCT image of a patient with an additional right PV and the visualization of the right PV with ICE.

EARLY BRANCHING. An early branching pattern of the right PV was observed in the majority (83%) of patients with MSCT, but was only recognized in 19 (45%) patients with ICE (sensitivity 19 of 35 [54%]). An early branching pattern of the left PV was observed in 5 (12%) with both MSCT and ICE.

COMMON OSTIA. Before entering the left atrium, often both left- and right-sided veins united in a short or long common trunk. Such a common ostium of the upper and lower PV was observed more often in the left PV with both techniques. Common ostia of left PV were observed in 33 (79%) patients with MSCT and in 31 (74%) patients with ICE. Common ostia of right PV were seen in 13 (31%) of patients with MSCT and in 16 (38%) of patients with ICE. In three cases, visualization of right-sided PV was laborious, and ostia appeared confluent. These patients were scored by the observers as common ostia, whereas separate ostia were identified using MSCT. Figure 5 (lower panel) demonstrates images obtained with MSCT and ICE in a patient with a common ostium of the left PV and of the right PV.

Quantitative measurements. Average measurements of pulmonary venous ostia in the anterior-posterior direction performed with MSCT were similar to measurements in the largest directions performed with ICE, except for measurements in the left inferior PV. When both left veins were compared with measurements performed with MSCT in the anterior-posterior direction, this difference was no longer significant. On the contrary, measurements performed with MSCT in superior-inferior directions were significantly larger than measurements performed with ICE in the largest direction (Table 2). The difference between all measurements performed with MSCT and with ICE was within two standard deviations from the average difference for most measurements, as was demonstrated with Bland-Altman analysis (Fig. 6).

Calculations of the venous ostium indexes (ratios of measurements of PV ostia in the anterior-posterior and in the superior-inferior direction), as measured with MSCT, demonstrated that the venous ostium indexes of the left PV were significantly smaller than the venous ostium indexes of the right PV, indicating a more oval shape of left PV ostia (Table 3). The diameters in the superior-inferior direction were significantly larger than the diameters in the anterior-posterior direction, indicating the long axis of the ostia to be in the superior-inferior direction (Table 2). Right-sided additional veins were significantly smaller than the "native" veins, and venous ostium indexes indicated a round shape of these ostia (1.02 ± 0.27). As the monoplane ICE transducer provides only 2-D images, multidimensional information cannot be obtained by ICE.

RFCA. Eventually 36 patients were treated with RFCA for PV isolation. In five patients, left-sided RFCA was not

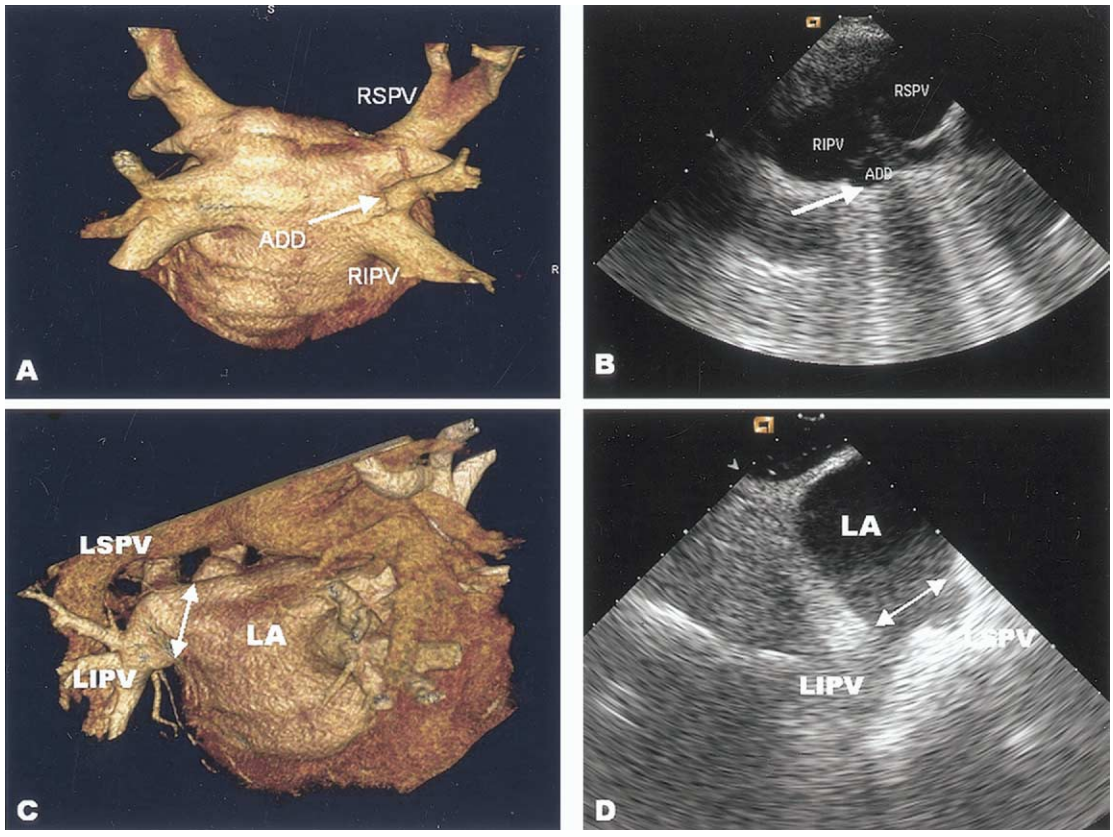

Figure 5. (Upper panels) Additional right pulmonary vein **(arrow)**, as observed with multislice computed tomography **(A)** and with intracardiac echocardiography **(B)**. **(Lower panels)** Common ostium **(double arrow)** of the left pulmonary veins, as observed with multislice computed tomography **(C)** and with intracardiac echocardiography **(D)**. Abbreviations as in Figure 1.

performed because of the presence of left atrial thrombus detected by ICE (two patients), the inability to perform transseptal puncture (one patient), and the induction of only atrial flutter (one patient) or atrial tachycardia (one patient), for which right atrial isthmus ablation and focal ablation of atrial tachycardia were performed, respectively. In one patient, the procedure was terminated because of recurrent strong vagal response with hypotension and severe bradycardia during the application of radiofrequency current. Procedural success was achieved in 34 of 36 (94%) patients. Mean procedure time was 252 ± 76 min, and mean fluoroscopy time was 49 ± 14 min. In three patients, mild pericardial effusion (<1.5 cm) was observed at the end of the procedure, without hemodynamic consequences. This effusion resolved on follow-up transthoracic echocardiography. No complications were observed during the first 48 h after the procedure. At six months follow-up, 23 of 36 (64%) patients were in sinus rhythm.

Table 2. Measurements of Ostia Pulmonary Veins: MSCT Versus ICE

	MSCT AP Diameters (mm)	MSCT SI Diameters (mm)	ICE Diameters (mm)	AP Diameter MSCT vs. ICE p Value	SI Diameter MSCT vs. ICE p Value
LSPV	14.6 ± 3.0	19.0 ± 3.8*	14.3 ± 3.9	NS	<0.01
LIPV	12.8 ± 3.0	17.1 ± 2.9*	14.3 ± 3.0	<0.01	<0.01
Both LPV	13.7 ± 3.1	18.0 ± 3.5*	14.3 ± 3.5	NS	<0.01
RSPV	16.5 ± 3.2	19.2 ± 2.8*	15.9 ± 4.7	NS	<0.01
RIPV	16.6 ± 3.9	18.2 ± 3.7*	15.4 ± 4.3	NS	<0.01
Both RPV	16.6 ± 3.6	18.7 ± 3.3*	15.7 ± 4.5	NS	<0.01
LCO	20.4 ± 7.5	26.8 ± 6.8*	24.3 ± 3.9	NS	NS
RCO	25.9 ± 7.5	33.5 ± 7.6*	21.6 ± 7.3	NS	<0.05
Additional RPV	7.4 ± 1.6	7.6 ± 2.0	8.5 ± 1.8	NS	<0.05
Additional LPV	11.0	10.1	—	—	—
All PV	15.1 ± 3.6	18.4 ± 3.4*	14.9 ± 4.0	NS	<0.01

*Significantly larger compared with AP diameters.

AP = anterior-posterior; ICE = intracardiac echocardiography; LCO = left common ostium; LIPV = left inferior pulmonary vein; LPV = left pulmonary veins; LSPV = left superior pulmonary vein; MSCT = multislice computed tomography; PV = pulmonary veins; RCO = right common ostium; RIPV = right inferior pulmonary vein; RPV = right pulmonary veins; RSPV = right superior pulmonary vein; SI = superior-inferior.

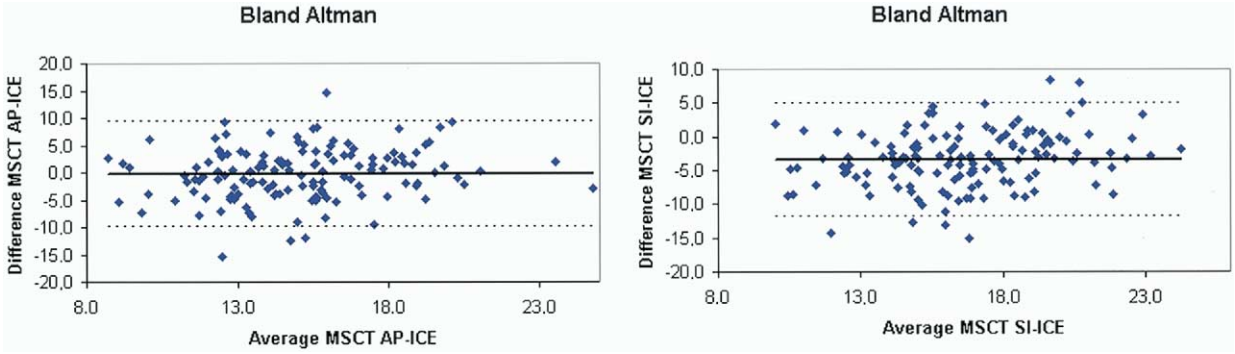

Figure 6. Bland-Altman analysis of measurements performed with multislice computed tomography (MSCT) and intracardiac echocardiography (ICE) in the anterior-posterior (AP) direction **(left panel)** and in the superior-inferior (SI) direction **(right panel)**. The difference between all measurements performed with MSCT and with ICE was within two standard deviations from the average difference for the majority of measurements.

DISCUSSION

In this study, we have compared the ability of MSCT and ICE to obtain both anatomic and quantitative information on the PV before RFCA. Considering MSCT as the gold standard, the main findings of this study are: 1) a higher sensitivity of MSCT to detect additional veins and right-sided early pulmonary venous branches, and 2) an underestimation of pulmonary venous ostial size using ICE.

Anatomic information. At present, there is no generally accepted definition which defines the exact border between the left atrial body and the PV. Also, data on the exact prevalence of PV variability are scarce. In general, common ostia are observed more frequently on the left side, whereas the presence of additional veins and early branching is described more often for right-sided veins (5,6,9–11), which agrees with data in the current study. Although variations in PV anatomy were observed with both MSCT and ICE, additional PV were observed more frequently with MSCT. Furthermore, an early branching pattern of right-sided PV was more often observed by MSCT. These data are in line with recent observations (12). In our experience, evaluation of the left-sided PV with ICE is more easily performed than evaluation of the right-sided veins. This may be attributed to the fact that the right-sided veins often make a sharp angle with the interatrial septum, thus limiting a longitudinal evaluation using the monoplane ICE transducer.

Knowledge of the existence of additional PV may have implications for the RFCA strategy. Because arrhythmogenic capacities have been demonstrated in additional right PV (13), targeting of these veins during RFCA procedures may improve procedural success rates.

Quantitative information. The main observations of quantitative data comparing both techniques demonstrated that the average measurements in the anterior-posterior direction performed with MSCT were similar to measurements performed in the largest direction with ICE. Furthermore, average ostial diameters in the superior-inferior direction as measured by MSCT were larger as compared with the monoplane measurements in the largest direction performed with ICE, indicating that ICE may underestimate the true ostial size in the largest direction. This hypothesis is supported by the fact that the venous ostium indexes (ratios of the measurements in two directions obtained by MSCT) were indicative of an oval shape of especially the left, and to a lesser extent the right, pulmonary venous ostia, with the long axis in the superior-inferior direction. These data agree with data reported by Witkampf et al. (11). Consequently, using a monoplane intracardiac ultrasound transducer, PV may appear smaller than their true dimensions. Intracardiac 3-D echocardiography may be a solution to this problem (14).

RFCA. An advantage from 3-D imaging with MSCT is the ability to accurately evaluate the pulmonary venous ostial dimensions before the ablation procedure, because the ostia can be observed in different orthogonal planes. Three-dimensional reconstructions of these images may provide a roadmap for targeting ablation points during RFCA, whereas information on ostial shape and size may also be useful to determine the size of Lasso catheters. Detailed knowledge of individual 3-D morphology of the PV may also contribute to an improved clinical success rate of PV

Table 3. Indexes of Diameters Measured in Anterior-Posterior and Superior-Inferior Direction of Pulmonary Venous Ostia, as Measured With MSCT

Vein	Index AP/SI Diameters
LSPV	0.79 ± 0.20*
LIPV	0.75 ± 0.16†
Both LPV	0.77 ± 0.18‡
RSPV	0.88 ± 0.13
RIPV	0.92 ± 0.16
Both RPV	0.90 ± 0.15
CO LPV	0.89 ± 0.63
CO RPV	0.82 ± 0.30
Additional LPV	1.09
Additional RPV	1.02 ± 0.27

*$p < 0.05$ vs. RSPV. †$p < 0.01$ vs. RIPV. ‡$p < 0.01$ vs. both RPV.

AP = anterior-posterior; CO = common ostium; LIPV = left inferior pulmonary vein; LPV = left pulmonary veins; LSPV = left superior pulmonary vein; MSCT = multislice computed tomography; RIPV = right inferior pulmonary vein; RPV = right pulmonary veins; RSPV = right superior pulmonary vein; SI = superior-inferior.

isolation (15). Additionally, ICE can be useful to exclude thrombus in the left atrial appendage, guide transseptal puncture, and provide on-line information on the position of catheters and PV hemodynamics pre and post RFCA. Some authors recommend the adjustment of radiofrequency power settings according to the appearance of microbubbles detected by ICE (7).

Besides MSCT and ICE, electro-anatomic mapping using 3-D non-fluoroscopic mapping systems has become an important tool for guiding electrophysiologic ablation procedures. These systems have the advantage that catheter navigation can be traced on-line and correlated to local electrograms (16,17). New technology is able to use computed tomographic information on-line (18), and a future application is the integration of activation maps on 3-D computed tomographic images and the fusion of real-time ICE images with images obtained by computed tomography/magnetic resonance imaging (19).

Conclusions. Variation in PV anatomy is frequently observed with both MSCT and ICE. The sensitivity for detection of additional branches and right-sided early branching is higher for MSCT. Measurements performed in the anterior-posterior direction using MSCT agree with measurements performed with ICE in the largest direction, whereas average measurements in the superior-inferior direction performed with MSCT are significantly larger then average measurements performed with ICE, suggesting underestimation of true ostial size by ICE. Three-dimensional imaging techniques, such as MSCT, are required to demonstrate an asymmetrical shape of PV ostia. The integration of MSCT data with on-line information obtained by ICE may optimize the treatment of atrial fibrillation by RFCA at PV ostia.

Reprint requests and correspondence: Dr. Jeroen J. Bax, Dept. of Cardiology, Leiden University Medical Center, Albinusdreef 2, 2333 ZA Leiden, the Netherlands. E-mail: jbax@knoware.nl.

REFERENCES

1. Haissaguerre M, Jais P, Shah DC, et al. Spontaneous initiation of atrial fibrillation by ectopic beats originating in the pulmonary veins. N Engl J Med 1998;339:659–66.
2. Haissaguerre M, Shah DC, Jais P, et al. Electrophysiological breakthroughs from the left atrium to the pulmonary veins. Circulation 2000;102:2463–5.
3. Haissaguerre M, Jais P, Shah DC, et al. Electrophysiological end point for catheter ablation of atrial fibrillation initiated from multiple pulmonary venous foci. Circulation 2000;101:1409–17.
4. Pappone C, Rosanio S, Oreto G, et al. Circumferential radiofrequency ablation of pulmonary vein ostia: a new anatomic approach for curing atrial fibrillation. Circulation 2000;102:2619–28.
5. Perez-Lugones A, Schvartzman PR, Schweikert R, et al. Three-dimensional reconstruction of pulmonary veins in patients with atrial fibrillation and controls: morphological characteristics of different veins. Pacing Clin Electrophysiol 2003;26:8–15.
6. Schwartzman D, Lacomis J, Wigginton WG. Characterization of left atrium and distal pulmonary vein morphology using multidimensional computed tomography. J Am Coll Cardiol 2003;41:1349–57.
7. Marrouche NF, Martin DO, Wazni O, et al. Phased-array intracardiac echocardiography monitoring during pulmonary vein isolation in patients with atrial fibrillation: impact on outcome and complications. Circulation 2003;107:2710–6.
8. Mangrum JM, Mounsey JP, Kok LC, DiMarco JP, Haines DE. Intracardiac echocardiography-guided, anatomically based radiofrequency ablation of focal atrial fibrillation originating from pulmonary veins. J Am Coll Cardiol 2002;39:1964–72.
9. Kato R, Lickfett L, Meininger G, et al. Pulmonary vein anatomy in patients undergoing catheter ablation of atrial fibrillation: lessons learned by use of magnetic resonance imaging. Circulation 2003;107:2004–10.
10. Scharf C, Sneider M, Case I, et al. Anatomy of the pulmonary veins in patients with atrial fibrillation and effects of segmental ostial ablation analyzed by computed tomography. J Cardiovasc Electrophysiol 2003;14:150–5.
11. Wittkampf FH, Vonken EJ, Derksen R, et al. Pulmonary vein ostium geometry: analysis by magnetic resonance angiography. Circulation 2003;107:21–3.
12. Wood MA, Wittkamp M, Henry D, et al. A comparison of pulmonary vein ostial anatomy by computerized tomography, echocardiography, and venography in patients with atrial fibrillation having radiofrequency catheter ablation. Am J Cardiol 2004;93:49–53.
13. Tsao HM, Wu MH, Yu WC, et al. Role of right middle pulmonary vein in patients with paroxysmal atrial fibrillation. J Cardiovasc Electrophysiol 2001;12:1353–7.
14. Smith SW, Light ED, Idriss SF, Wolf PD. Feasibility study of real-time three-dimensional intracardiac echocardiography for guidance of interventional electrophysiology. Pacing Clin Electrophysiol 2002;25:351–7.
15. Ernst S, Antz M, Ouyang F, et al. Ostial PV isolation: is there a role for three-dimensional mapping? Pacing Clin Electrophysiol 2003;26:1624–30.
16. Macle L, Jais P, Scavee C, et al. Pulmonary vein disconnection using the LocaLisa three-dimensional nonfluoroscopic catheter imaging system. J Cardiovasc Electrophysiol 2003;14:693–7.
17. Nademanee K, McKenzie J, Kosar E, et al. A new approach for catheter ablation of atrial fibrillation: mapping of the electrophysiologic substrate. J Am Coll Cardiol 2004;43:2044–53.
18. Solomon SB, Dickfeld T, Calkins H. Real-time cardiac catheter navigation on three-dimensional CT images. J Interv Card Electrophysiol 2003;8:27–36.
19. Packer DL. Evolution of mapping and anatomic imaging of cardiac arrhythmias. J Cardiovasc Electrophysiol 2004;15:839–54.